PCCP

Accepted Manuscript

This is an *Accepted Manuscript*, which has been through the Royal Society of Chemistry peer review process and has been accepted for publication.

Accepted Manuscripts are published online shortly after acceptance, before technical editing, formatting and proof reading. Using this free service, authors can make their results available to the community, in citable form, before we publish the edited article. We will replace this *Accepted Manuscript* with the edited and formatted *Advance Article* as soon as it is available.

You can find more information about *Accepted Manuscripts* in the **Information for Authors**.

Please note that technical editing may introduce minor changes to the text and/or graphics, which may alter content. The journal's standard **Terms & Conditions** and the **Ethical guidelines** still apply. In no event shall the Royal Society of Chemistry be held responsible for any errors or omissions in this *Accepted Manuscript* or any consequences arising from the use of any information it contains.

Molybdenum Disulfide as a Highly Efficient Absorbent for Non-polar Gases

Ningning Yu, Lu Wang[*], Min Li, Xiaotian Sun, Tingjun Hou, Youyong Li[*]

Molybdenum disulfide, a kind of graphene-like two-dimensional material, has attracted great interests due to its unique properties with potential applications in electronics and sensors. Here, we perform first-principles calculations and grand canonical Monte Carlo (GCMC) simulations and show that MoS_2 layer is efficient to absorb non-polar gases. Compared with the popular gas sorbents (MOFs and carbon-based materials), MoS_2 exhibits additional advantages, including large surface to volume ratio and tunable properties. We systematically study the non-polar gases (CO_2 and CH_4) adsorption on MoS_2 layer with and without vacancies. The perfect MoS_2 shows little or no adsorption for CO_2 and CH_4 molecules, but the MoS_2 with single S vacancy and double S vacancies exhibit excellent adsorption ability for CO_2 and CH_4 gases. The absorption energies are 65 kJ/mol for CO_2 and 47 kJ/mol for CH_4 (vdW-D2), respectively. An orbital coupling between the p orbital of CO_2 (or CH_4) molecule and the d orbital of Mo atom is observed. GCMC simulation results show that MoS_2 with single S vacancy could absorb 42.1wt% CO_2 and 37.6wt% CH_4 under the pressure of 80 Bar at the room temperature. Our results indicate that monolayer MoS_2 with defects is a highly efficient absorbent for non-polar gases.

1. INTRODUCTION

Release of industrial and vehicle exhaust gases into atmosphere is one of the major sources of the current environmental problems. Among the exhaust gases, carbon dioxide (CO_2) and methane (CH_4) are the main gases that cause the warming effect. So, finding ideal sorbents for effective gas capture is a crucial issue in the energy and environmental science. Due to the inert property of non-polar CO_2 and

Functional Nano & Soft Materials Laboratory (FUNSOM), Soochow University, Suzhou, 215123 Jiangsu, China. Email: lwang22@suda.edu.cn and yyli@suda.edu.cn

CH_4 gases, most of the materials show a weak adsorption and are not sensitive to capture them. Up to

now, different sorbents have been tried for CO_2 and CH_4 capture, such as MOF[1-3], COF[4, 5], zeolites[6, 7]

and carbon-based nanomaterial[8-11]. For example, MOF-5, MOF-177 and zeolite 5A have been used as

the sorbents for CO_2 and CH_4 adsorption, and the adsorption capacity for CH_4 and CO_2 can be as high

as 22 wt% on MOF-177 at 298K and 100 Bar and 47.98 wt% on MOF-5 at 298K and 14 bar,

respectively. [3]

As the rise of graphene, graphene-like two-dimensional (2D) materials have attracted great interests

recently. Monolayer molybdenum disulfide (MoS_2), a kind of transition metal dichalcogenide (TMD)

material, is a well-established semiconductor with a direct band gap of 1.9 eV[12]. Unlike graphene,

monolayer MoS_2 is constructed by triple atomic layers, in which Mo atoms are sandwiched between

two S atoms. Due to its unique electronic, optical, and chemical properties, MoS_2 has been extensively

investigated both experimentally[13-21] and theoretically.[22, 23] It is recognized as a promising candidate for

novel electronics and photonics devices. For example, monolayer MoS_2 has been successfully

synthesized to be used as the channel material in a field-effect transistor with a high channel mobility

of ~200 $cm^2V^{-1}s^{-1}$ and current on/off ratio of 1×10^8 at the room temperature[24]. After that, a

phototransistor based on the monolayer MoS_2 is fabricated by Zhang's group, and photocurrent

generation and annihilation can be switched within ca. 50 ms, which exhibits a better photoresponsivity

compared to the graphene-based device[25].

Since possessing a high surface-to-volume ratio and flexible properties compared to graphene-based

materials, MoS_2 layer is expected to be efficient gas sorbents or sensors. The field-effect transistors

(FET) based on single- and multi-layer MoS_2 films have been successfully synthesized recently, which

can be used as gas sensors to detect nitrous oxide (NO) with a detection of 0.8 ppm[26]. In addition, the

superior sensitivity for nitrous dioxide (NO_2) has been observed in a flexible FET sensor array based on

a MoS_2 channel and reduced graphene oxide electrodes[27]. Though some experimental results indicated

that MoS_2 holds great promise for gas sensors, the underlying adsorption mechanism for different gases

is not very clear and the theoretical studies is limited[28].

Here we explore the response of monolayer MoS_2 with and without vacancies to non-polar gas

molecules (CO_2 and CH_4) using first-principles calculations combined with grand canonical Monte

Carlo (GCMC) method. Recently, Zhou et al. have observed various structural defects in chemical

vapor phase grown monolayer MoS_2 by direct atomic resolution imaging, including point defects,

dislocations, grain boundaries and edges[29]. Among these point defects, the single vacancy of S is

frequently observed in experiments, which indicates its stability. These defective sites are reactive and

could influence the electronic properties, so here we consider the monolayer MoS_2 with point defects

for the gas adsorption. Our results confirm that monolayer MoS_2 with defect is a highly efficient

absorbent for non-polar gases.

2. METHOD

All computations are performed using all-electron density functional theory (DFT) with a double

numerical basis set plus polarization functions (DNP), as implemented in the $DMol^3$ program[30]. The

generalized gradient approximation (GGA) with Perdew−Burke−Ernzerhof (PBE) exchange −

correlation functional including van der Waals (vdW) corrections (DFT-D2 Grimme's method) was

adopted[31]. Self-consistent field (SCF) computations were performed with a convergence criterion of

10^{-5}a.u. for the total energy. To make sure to get the high-quality numerical results, we chose the

real-space global orbital cutoff radius as high as 5.5 Å in all computations without symmetry constraint. A 6×6 supercell of hexagonal MoS_2 unit cell was used to study the defective structures and gas adsorption. The supercell dimension for the direction perpendicular to the MoS_2 layer is chosen as 15 Å to avoid the interaction between neighboring layers. During the geometry optimization, the k space was sampled by the Gamma point in the Brillouin zone, and the Monkhorst–Pack grids with separation of 0.03 Å were chosen.

The adsorption energy for CO_2 and CH_4 molecules on the monolayer MoS_2 with and without vacancies is defined by

$$E_a = E_{gas\text{-}MoS_2} - E_{MoS_2} - E_{gas} \qquad (1)$$

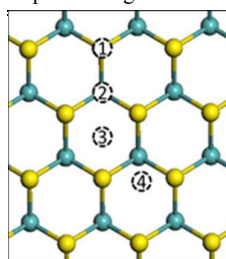where $E_{gas\text{-}MoS_2}$ represents the total energy of the complexes of gases and MoS_2 substrates, E_{MoS_2} and E_{gas} are the total energies of the MoS_2 substrate and the adsorbed gas molecules, respectively. A negative value of E_a indicates that the gas molecule prefers to adsorb on the substrate, while a positive value of E_a means a repulsion interaction between the gas molecule and the substrate.

The gas adsorption properties were simulated using the grand canonical Monte Carlo method, which implemented in Sorption module in Materials Studios 7.0. During GCMC simulations, the MoS_2 sorbent were assumed to be rigid with constraint atoms. The van der Waals (vdW) interactions between the gas molecules and the MoS_2 sheet are described by the Universal force field[32] but with the revised Lennard-Jones (LJ) parameters obtained from our first-principles calculations. We carried out a series of fixed pressure simulations at the room temperature of 298 K from 0 to 80 bar. At each pressure, the GCMC simulation consisted of 1×10^6 steps to allow equilibration, followed by 1×10^7 steps to sample the configuration space.

3. RESULTS AND DISCUSSION

3.1 CO_2 and CH_4 adsorption on perfect MoS_2 layer

TABLE I. Adsorption energies and distances for gas molecules adsorbed on perfect MoS_2 layer at different sites.

| Site	CO_2		CH_4	
	E_a (kJ/mol)	d (Ă)	E_a (kJ/mol)	d (Ă)
(1) T-S	-6.9	3.40	10.1	3.41
(2) T-Mo	-10.2	2.90	8.5	3.76
(3) Hollow	-9.6	3.16	8.6	3.78
(4) B-2S	-9.3	3.04	8.7	3.54

Four geometric sites have been considered for the gas molecules (CO_2 and CH_4) adsorbed on perfect MoS_2 layer: 1) top S site, 2) top Mo site, 3) hollow site at the center of a hexagonal ring, and 4) bridge site between two neighboring S atoms in the same layer. TABLE I summarizes the gas adsorption energies and distances for both CO_2 and CH_4 molecules adsorbed on perfect MoS_2 layer at different sites. For CO_2, the adsorption energies on these four sites are all negative with the similar values, which indicates that it prefers to adsorb on MoS_2 surface without site dependence, but the adsorption energies are very small (less than 0.1 eV). On the other hand, the values of adsorption energies for CH_4 are all positive, which means that there is a repulsion interaction between CH_4 and MoS_2 layer. Among these four sites, the distances between CO_2 (or CH_4) and the Mo atom for the T-Mo site are (2.901 Å for CO_2 and 2.792 Å for CH_4, respectively) shorter than the others (more than 3.1 Å). Therefore, our results show that the perfect MoS_2 is not a suitable sorbent for non-polar gas adsorption, especially for CH_4 molecule.

3.2 CO_2 and CH_4 adsorption on MoS_2 with vacancies

The structural defects on MoS_2 layer has been observed and extensively investigated recently[15, 20, 29, 33]. The results show that the defective sites in MoS_2 layer are reactive and could influence the

electronic properties. Thus, here we propose to use the monolayer MoS_2 with point defects as the sorbent for the non-polar gas molecules adsorption. We considered five types of defective structures including single vacancy of missing one S (S-SV), single vacancy of missing one Mo (Mo-SV), double vacancies by missing one Mo and one S (Mo-S-DV), double vacancies by missing two S (2S-DV) and 585 defect by missing a MoS_2 unit. The optimized configurations are shown in FIG. 1. The defect formation energies are calculated using the Brenstone as the reservoirs at the experimental condition of S rich. From the results, the S-SV defect is found to show the lowest formation energy of 3.03 eV, while the 585 defect with missing a MoS_2 unit possesses the highest formation energy of 7.61 eV under S-rich environment. This is consistent with the experimental observations[29] and other theoretical calculations[28], where S-SV is frequently observed, and other defects were only occasionally found. In the S-SV structure, three Mo atoms at the vacancy site move closer to each other and form a small triangle like structure. The neighbor Mo–Mo bond lengths ($d_{Mo–Mo}$) become 3.055 Å, shorter than that in the perfect MoS_2 sheet (3.166 Å). Thus, the formation energy was lowered significantly due to the formation of three additional Mo–Mo bonds by removing of an S atom. And it is the same mechanism for the S-DV structure. On the other hand, in the Mo-SV, the three S atoms at the vacancy site move apart from each other and form a large triangle-like structure after optimization. And so does the S-Mo-DV structure. When one MoS_2 unit is missed, there will be two pentagonal rings and one octagonal ring forming the 585 defect, which possesses the highest formation energy.
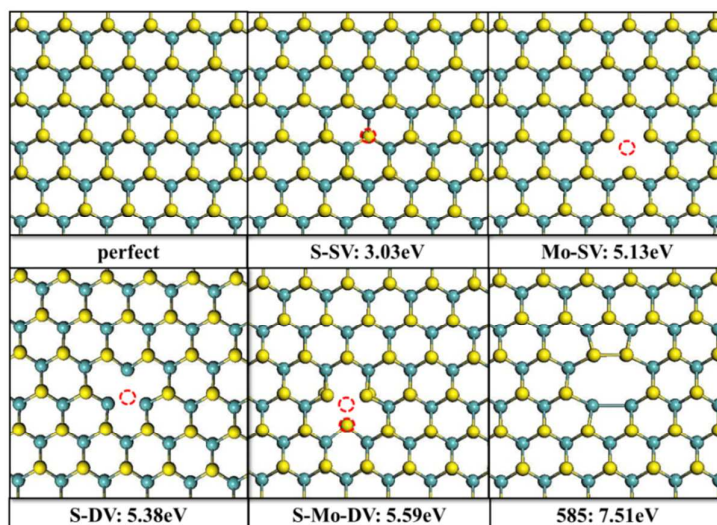
FIG. 1. Optimized structures and formation energies of (a) perfect MoS_2 and MoS_2 with (b) S-SV, (c) Mo-SV, (d) S-DV, (e) S-Mo-DV and (f) 585 defects.

Then, we calculated the adsorption properties of CO_2 and CH_4 molecules on the MoS_2 layer with these vacancies. TABLE II summarizes the adsorption energies, adsorption distances and charge transfer between the adsorbed gas molecules and the MoS_2 layer. The adsorption distance is defined by the vertical distance between the C atom in CO_2 or CH_4 molecules and the top S-layer of the MoS_2 sheet. We found that the adsorption energies for CO_2 and CH_4 on the MoS_2 sheet with S-SV defect can be as high as -65.8 kJ/mol for CO_2 and -47.6 kJ/mol for CH_4, respectively, which are much stronger than these gases adsorbed on some MOFs or carbon-based nanomaterials.[3, 9] The S-DV defect also possesses high adsorption energies close to S-SV defect, which are -64.1 kJ/mol for CO_2 and -45.2 kJ/mol for CH_4, respectively. The adsorption distances for these two defects are around 2.5 Å, which are shorter than the other defects. For CO_2, S-Mo-DV and 585 defect structures give the moderate adsorption energies of -20.5 kJ/mol and -26.9 kJ/mol, respectively, while Mo-SV structure shows the lowest adsorption energy of -9.4 kJ/mol, comparable to that on perfect MoS_2 layer. FIG. 2 shows the adsorption configuration of CO_2 adsorbed on MoS_2 with and without defects. There are two types of configurations for CO_2, one is the linear CO_2 molecule perpendicular to the surface of MoS_2 layer, and

the other is the linear CO_2 molecule tilts with the O atom pointing to the S defect. For CH_4, the 585

defect structure gives a low adsorption energy of -5.1 kJ/mol, while both Mo-SV and S-Mo-DV

structures show the repulsive interaction with the CH_4 molecule as the perfect MoS_2 layer. From the

Mulliken population analysis, the charge transfer between CO_2 (or CH_4) molecules and the S-SV and

S-DV defects are relatively larger than the others, which is further proved that the gas molecules give a

stronger interacting with S-SV and S-DV defects.

TABLE II. Adsorption energies (E_a), adsorption distances (d) and the Mulliken charge transfer (Q) between gas molecules and MoS_2 with and without defects.

| Structures	CO_2			CH_4		
	E_a (kJ/mol)	d (Å)	Q (e)	E_a (kJ/mol)	d (Å)	Q (e)
perfect	-10.2	3.22	0	8.9	3.23	0
S-SV	-65.8	3.04	0.020	-47.6	2.58	0.041
Mo-SV	-9.4	3.24	0	8.7	3.30	0
2S-DV	-64.1	3.20	0.021	-45.2	2.50	0.058
S-Mo-DV	-20.5	2.52	0.013	10.1	3.20	0
585	-26.9	2.79	0.018	-5.1	2.75	0.020
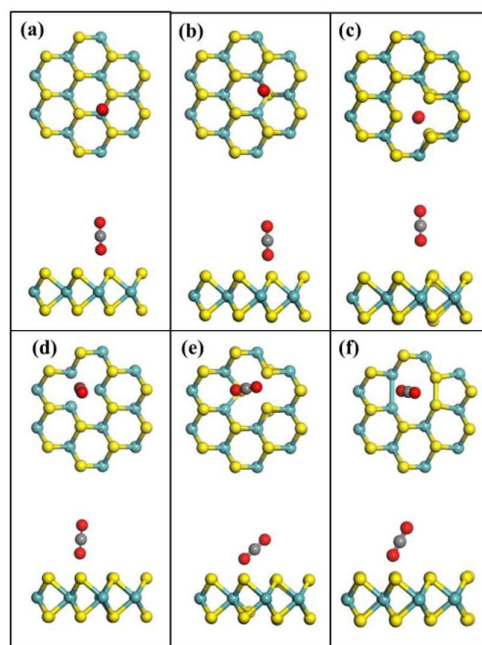
FIG. 2. Top view and side view for CO_2 molecule adsorbed on (a) perfect MoS_2 and MoS_2 with (b) S-SV, (c) Mo-SV, (d) S-DV, (e) S-Mo-DV and (f) 585 defects.

To investigate the interaction between gas molecules and the MoS_2 layer, we analyzed the projected

electronic density of states (PDOS) for the d orbital of Mo atoms near the vacancy site and the s and p

orbitals of gas molecules. FIG. 3 shows the PDOS and the deformation charge density for CO_2 and CH_4

molecules adsorbed on MoS_2 with S-SV defect. When a CO_2 (or CH_4) molecule adsorbs on the vacancy

site, there is an orbital coupling between the p orbital of CO_2 (or CH_4) molecule and the d orbital of Mo

atom. The deformation charge density is also calculated for CO_2 and CH_4 molecules adsorbed on MoS_2

with S-SV and S-DV defects. The differential charge (ΔQ) is defined as

$$\Delta Q = Q(gas\text{-}MoS_2) - Q(MoS_2) - Q(gas) \tag{2}$$

where $Q(gas\text{-}MoS_2)$, $Q(MoS_2)$ and $Q(gas)$ are the charge density for the gas-MoS_2 system, MoS_2

substrate and a gas molecule, respectively. The deformation charge density for CO_2 and CH_4 molecules

adsorbed on MoS_2 with S-SV is plotted in Fig. 3(b)-(d), which indicates a Van der Waals interaction

with polarization of the gas molecules and the MoS_2 substrate. The charge difference distributes in the

middle region between the gas molecules (CO_2 and CH_4) and the MoS_2 substrate, suggesting partly

covalent character. Therefore, the interactions between the gas molecules and the MoS_2 with S-SV

defect are mainly weak van der Waals interaction with partly covalent character. This hybrid interaction

is also observed when the gas molecules adsorbed on the S-DV site of MoS_2 substrate, which is plotted

in Fig. S1 of Supplementary Information.
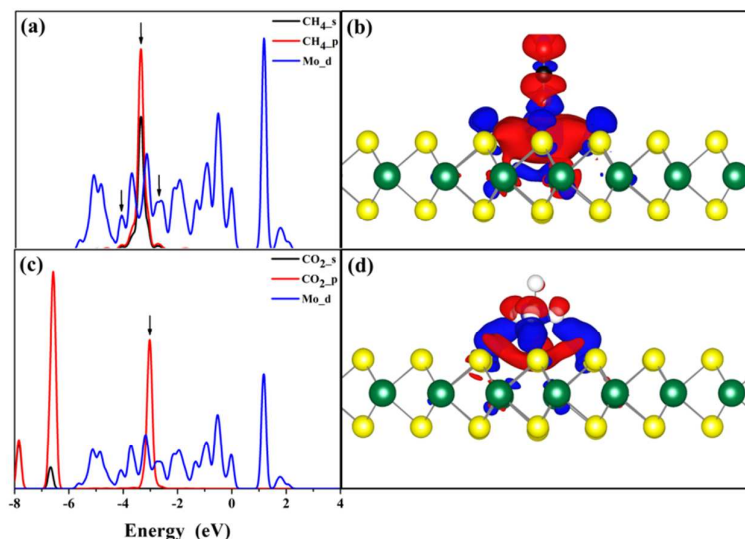
FIG. 3. The projected density of states (PDOS) for the *d* orbital of Mo and the *s* and *p* orbitals of (a) CH_4 and (c) CO_2; (b) and (d) are the deformation charge density for CO_2 and CH_4 adsorbed on MoS_2 layer with S-SV defect. The increase and decrease of the electron density are colored in red and blue, respectively.

3.3 Gas adsorption isotherms

To determine the capability of MoS_2 with vacancies as absorbent for CO_2 / CH_4, we perform GCMC (grand canonical Monte Carlo) calculations. The calculated gravimetric adsorption isotherms of the CO_2 and CH_4 molecules on MoS_2 layer with S-SV defect at room temperature (298 K) are plotted in FIG. 4a-b as an example. We can see that the adsorption increases with the pressure increasing and gradually approaches saturation, which indicates the stronger adsorption. The adsorption amount of CH_4 is much more than that of CO_2 on MoS_2 with S-SV defect, for example, 29.3wt% for CH_4 and 28.6wt% for CO_2 at the pressure of 16 bar and 35.2wt% for CH_4 and 38wt% for CO_2 at 40 bar, respectively. Finally, the adsorption amount of CH_4 and CO_2 reaches to 37.6wt% and 42.1wt% at the pressure of 80 bar and the room temperature, respectively. We also investigate the density distribution of the CH_4 and CO_2 molecules adsorbed on the MoS_2 with S-SV defect. FIG. 4c-d shows the top view and side view of adsorption density distribution for CH_4 molecules on MoS_2 with S-SV defect as an

10

example at 80 bar. Obviously, the CH_4 molecules are not distributed uniformly, but congregate around

the defective sites, which is consistent with our first-principles calculations. The same phenomenon is

also observed for CO_2 molecule (see Fig. S2 in Supplementary Information). Therefore, the MoS_2 with

defects can be used as an efficient absorbent for non-polar gas molecules, and the adsorption capability

can be modulated by the density of defects in MoS_2 layer. Since in experiments, bilayer and multilayer

of MoS_2 are commonly synthesized and have enough space between layers for gas molecules to access,

we speculate that multilayer MoS_2 can be more effective at capturing these gases and these calculations

are currently in progress.
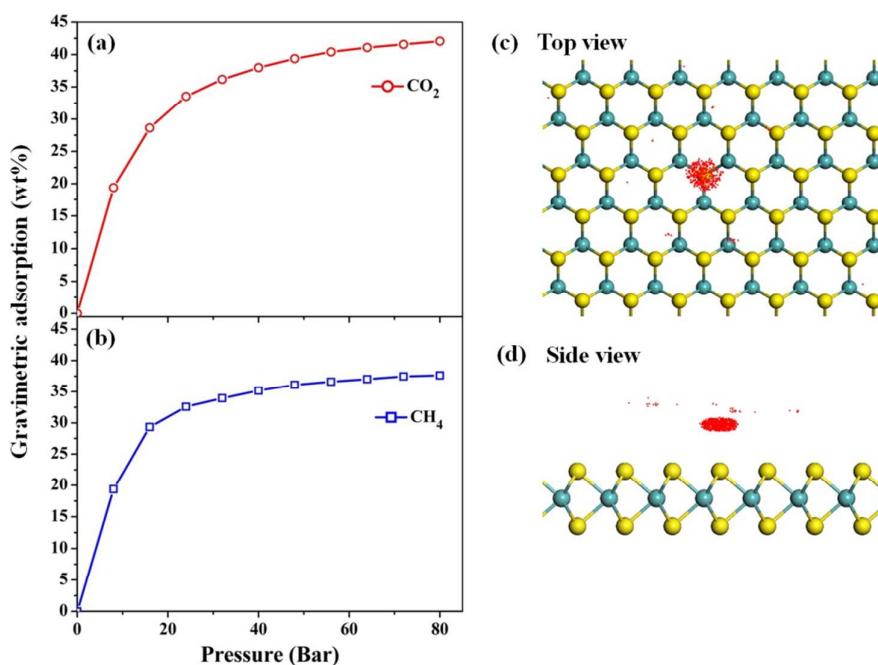
FIG. 4. The adsorption isothermals for (a) CH_4 and (b) CO_2 on monolayer MoS_2 with S-SV defect at 298K; (c) and (d) are the top view and side view of adsorption density distribution for CH_4 molecules on MoS_2 with S-SV defect at 80 bar, respectively.

4. CONCLUSION

In this work, we systematically investigated the adsorption properties for non-polar gas molecules (CO_2

and CH_4) on perfect monolayer MoS_2 and MoS_2 with vacancies by first-principles calculations

combined with GCMC simulations. Perfect MoS_2 lacks the adsorption ability for these non-polar gases, but MoS_2 with point defects especially the S vacancy displays good adsorption behavior with the large adsorption energies of 65 kJ/mol for CO_2 and 47 kJ/mol for CH_4, respectively. Density of states and deformation charge density analysis show that the interactions between the gas molecules and the MoS_2 layer with vacancies are mainly weak van der Waals interaction with some covalent character. Our GCMC calculations predict a high adsorption amount of 42.1wt% for CO_2 and 37.6wt% for CH_4 on MoS_2 with single S vacancy under the pressure of 80 bar at the room temperature, respectively. Our results indicate that monolayer MoS_2 with defects is a highly efficient absorbent for non-polar gases.

REFERENCES

1 S. Hermes, M. K. Schroter, R. Schmid, L. Khodeir, M. Muhler, A. Tissler, R. W. Fischer and R. A. Fischer, Angew. Chem. *Int. Ed. Engl*, 2005, **44**, 6237.

2 Y. Li and R. T. Yang, *Langmuir*, 2007, **23**, 12937.

3 D. Saha, Z. Bao, F. Jia and S. Deng, *Envir. Sci. Technol*, 2010, **44**, 1820.

4 Y. Liu, D. Liu, Q. Yang, C. Zhong and J. Mi, *Ind. Eng. Chem. Res*, 2010, **49**, 2902.

5 S. S. Han, H. Furukawa, O. M. Yaghi and W. A. Goddard Iii, *J. Am. Chem. Soc*, 2008, **130**, 11580.

6 J. Vermesse, D. Vidal and P. Malbrunot, *Langmuir*, 1996, **12**, 4190.

7 R. Krishna and J. M. van Baten, *Langmuir*, 2010, **26**, 3981.

8 F. Schedin, A. K. Geim, S. V. Morozov, E. W. Hill, P. Blake, M. I. Katsnelson and K. S. Novoselov, *Nat. Mat*, 2007, **6**, 652.

9 B. Huang, Z. Li, Z. Liu, G. Zhou, S. Hao, J. Wu, B.-L. Gu and W. Duan, *J. Phys. Chem. C*, 2008, **112**, 13442.

10 R. Arsat, M. Breedon, M. Shafiei, P. Spizziri, S. Gilje, R. Kaner, K. Kalantar-zadeh and W. Wlodarski, *Chem. Phys. Lett*, 2009, **467**, 344.

11 L. Wang, J. Zhao, L. Wang, T. Yan, Y.-Y. Sun and S. B. Zhang, *Phys. Chem. Chem. Phys*, 2011, **13**, 21126.

12 K. F. Mak, C. Lee, J. Hone, J. Shan and T. F. Heinz, *Phys. Rev. Lett*, 2010, **105**, 136805.

13 A. Castellanos-Gomez, R. Roldan, E. Cappelluti, M. Buscema, F. Guinea, H. S. van der Zant and G. A. Steele, *Nano lett*, 2013, **13**, 5361.

14 H. J. Conley, B. Wang, J. I. Ziegler, R. F. Haglund, Jr., S. T. Pantelides and K. I. Bolotin, *Nano lett*, 2013, **13**, 3626.

15 H.-P. Komsa, S. Kurasch, O. Lehtinen, U. Kaiser and A. V. Krasheninnikov, *Phys. Rev. B*, 2013, **88,** 035301.

16 Y. Li, H. Wang, L. Xie, Y. Liang, G. Hong and H. Dai, *J. Am. Chem. Soc*, 2011, **133**, 7296.

17 X. Liu, T. Xu, X. Wu, Z. Zhang, J. Yu, H. Qiu, J. H. Hong, C. H. Jin, J. X. Li, X. R. Wang, L. T. Sun and W. Guo, *Nature Commun*, 2013, **4**, 1776.

18 Y. Liu, L. Jiao, Q. Wu, Y. Zhao, K. Cao, H. Liu, Y. Wang and H. Yuan, *Nanoscale*, 2013, **5**, 9562.

19 Y. Shi, J. K. Huang, L. Jin, Y. T. Hsu, S. F. Yu, L. J. Li and H. Y. Yang, *Sci. Rep*, 2013, **3**, 1839.

20 J. Xie, H. Zhang, S. Li, R. Wang, X. Sun, M. Zhou, J. Zhou, X. W. Lou and Y. Xie, *Adv. Mater*, 2013, **25**, 5807.

21 C. R. Zhu, G. Wang, B. L. Liu, X. Marie, X. F. Qiao, X. Zhang, X. X. Wu, H. Fan, P. H. Tan, T. Amand and B. Urbaszek, *Phys. Rev. B*, 2013, **88**,121301.

22 S. Yang, D. Li, T. Zhang, Z. Tao and J. Chen, *J. Phys. Chem. C*, 2012, **116**, 1307.

23 Q. Yue, S. Chang, J. Kang, X. Zhang, Z. Shao, S. Qin and J. Li, *J. Phys-Condens. Mat*, 2012, **24**, 335501.

24 B. Radisavljevic, A. Radenovic, J. Brivio, V. Giacometti and A. Kis, *Nature Nanotech*, 2011, **6**, 147.

25 Z. Yin, H. Li, H. Li, L. Jiang, Y. Shi, Y. Sun, G. Lu, Q. Zhang, X. Chen and H. Zhang, *ACS nano*, 2011, **6**, 74.

26 H. Li, Z. Yin, Q. He, H. Li, X. Huang, G. Lu, D. W. H. Fam, A. I. Y. Tok, Q. Zhang and H. Zhang, *Small*, 2012, **8**, 63.

27 Q. He, Z. Zeng, Z. Yin, H. Li, S. Wu, X. Huang and H. Zhang, *Small*, 2012, **8**, 2994.

28 Q. Yue, Z. Shao, S. Chang and J. Li, *Nanoscale Res. Lett*, 2013, **8**, 1.

29 W. Zhou, X. Zou, S. Najmaei, Z. Liu, Y. Shi, J. Kong, J. Lou, P. M. Ajayan, B. I. Yakobson and J. C.

Idrobo, *Nano Lett*, 2013, **13**, 2615.

30 B. Delley, Comp. *Mater. Sci*, 2000, **17**, 122.

31 S. Grimme, *J. Comp. Chem*, 2006, **27**, 1787.

32 A. K. Rappé, C. J. Casewit, K. Colwell, W. Goddard Iii and W. Skiff, *J. Am. Chem. Soc*, 1992, **114**, 10024.

33 A. N. Enyashin, M. Bar-Sadan, L. Houben and G. Seifert, *J. Phys. Chem. C* , 2013,**117**, 10842.